Earth and Planetary Science Letters 301 (2011) 213–221

Contents lists available at ScienceDirect

Earth and Planetary Science Letters

journal homepage: www.elsevier.com/locate/epsl

A lithium isotopic study of sub-greenschist to greenschist facies metamorphism in an accretionary prism, New Zealand

Lin Qiu [a,*], Roberta L. Rudnick [a], Jay J. Ague [b], William F. McDonough [a]

[a] Department of Geology, University of Maryland, College Park, MD 20742, USA
[b] Department of Geology and Geophysics, Yale University, New Haven, CT, 06520, USA

ARTICLE INFO

Article history:
Received 30 June 2010
Received in revised form 25 October 2010
Accepted 1 November 2010
Available online 26 November 2010

Editor: R.W. Carlson

Keywords:
lithium
slab-derived fluids
accretionary prism
quartz veins
sub-greenschist facies
greenschist facies

ABSTRACT

To investigate the behavior of Li during low-grade metamorphism and fluid flux in an accretionary prism we measured the Li concentrations ([Li]) and isotopic compositions (δ^7Li) of sub-greenschist and greenschist-facies Otago Schist composites, as well as cross-cutting quartz veins, which are interpreted to have precipitated from slab-derived fluids. The average [Li] of sub-greenschist facies composites (41 ± 13 μg/g, 2σ) is statistically distinct (97% confidence level, student t test) to that of greenschist facies composites (34 ± 9 μg/g, 2σ), which have experienced mass addition of silica in the form of quartz veins having [Li] between 0.4–2.3 μg/g. A linear regression of the correlation between [Li] and calculated mass additions suggests that the depletion of [Li] in greenschist facies composites is due to both dilution from the addition of the quartz veins, as well as metamorphic dehydration. The [Li] of both groups of composites correlates with their CIA (Chemical Index of Alteration) values (50–58), which are low, consistent with the inferred graywacke protolith of the Otago Schist. The δ^7Li of sub-greenschist and greenschist facies composites are remarkably constant, with an average δ^7Li of 0.2 ± 1.7 (2σ) and -0.5 ± 1.9 (2σ), respectively, and comparable to that of the average upper continental crust. Thus, metamorphism has had no discernable effect on δ^7Li in these samples. The Li isotopic signature of the schists is similar to that seen in pelitic sedimentary rocks and likely reflects the δ^7Li of the protoliths. The surprisingly light δ^7Li of the quartz veins (-2.8 to -1.4) likely records kinetic fractionation associated with Li ingress into the veins from surrounding wallrock.

An isotopic equilibrium fluid flow model indicates that: 1) if the [Li] of slab-derived fluids is less than a few μg/g, the δ^7Li of the overlying lithologies (i.e., the schists) is not significantly influenced by the fluid flux, regardless of the δ^7Li of the fluids, 2) the slab-derived fluids will have heavy δ^7Li of $> +10$ after reacting with the prism sediments during their ascent, and 3) the [Li] of the slab-derived fluids is likely in the range of $0 < [\text{Li}] \leq 41$ (μg/g). Thus, isotopically heavy slab-derived fluids that traverse sediments in accretionary prisms may leave little trace in the rocks and their surface compositional characteristics will reflect the net result of their interaction with the sediments of the prism.

Published by Elsevier B.V.

1. Introduction

The fluid-mobile element lithium increasingly receives attention because of the large isotopic fractionation in δ^7Li that can occur at the Earth's surface and its possible usefulness as a tracer of crustal recycling in subduction zones (e.g., Elliott et al., 2004, 2006 and references therein). Nevertheless, Li isotopic fractionation during low-grade metamorphism, particularly during subduction-zone metamorphism, remains a matter of debate (e.g., Marschall et al., 2007; Zack et al., 2003).

Recent findings reveal that metamorphic dehydration has had little discernible effect on δ^7Li, even in the presence of lithium depletion (Marschall et al., 2007; Qiu et al., 2009; Teng et al., 2007). For example, the Li isotopic compositions of mudrocks from basins in the British Caledonides are unaffected by sub-greenschist facies metamorphism and reflect the Li isotopic signature of the protoliths (Qiu et al., 2009). However, metamorphism in the British mudrocks occurred at shallow depths, where initial dewatering occurs and pore water in the sediments dominates the fluid flux. Fluid flux and metamorphism occurring at deeper levels within accretionary prisms may be more complex. For example, greenschist facies metamorphism in an accretionary prism can be accompanied by ingress of large volumes of fluids derived from metamorphic dehydration of the subducting slab. These fluids may interact with the overlying metamorphic rocks to form quartz veins (Breeding and Ague, 2002; Kerrich, 1999, Smith and Yardley, 1999).

To date, the signature of Li in greenschist facies metamorphic rocks from accretionary prisms and associated fluid fluxing have not been investigated. Here, we report the Li concentrations and isotopic compositions of the Otago Schist, New Zealand, which constitutes a

* Corresponding author. Tel.: +1 240 413 4788; fax: +1 301 405 3597.
E-mail addresses: linqiu@geol.umd.edu (L. Qiu), jay.ague@yale.edu (J.J. Ague).

0012-821X/$ – see front matter. Published by Elsevier B.V.
doi:10.1016/j.epsl.2010.11.001

typical sequence of sub-greenschist to highly veined greenschist facies meta-graywackes and metapelites that formed in an accretionary prism (Bishop, 1972; Mortimer, 1993; Rahl et al., 2011). The results from this study offer insights into the behavior of Li during low-grade metamorphism, the factors controlling the Li isotopic composition of accretionary prism sedimentary rocks and, for the first time, provide information about the behavior of Li during fluid fluxing in an accretionary prism.

2. Geological background and samples

The Otago Schist is one of the three geographically discrete units of the Mesozoic Haast Schist belt, New Zealand; the other two are the Marlborough and Alpine Schists. The Otago Schist, comprising the Permian–Cretaceous Torlesse and Caples terranes (Fig. 1), forms an approximately 150-km-wide structural arch, with prehnite–pumpyllyite facies on the two outer flanks and greenschist facies in the center. The protoliths of the schist, principally graywacke–mudstone turbidites, were deposited and metamorphosed during subduction (Mortimer, 2000, 2003) and the burial and exhumation processes in the accretionary prism are recorded in these regional metamorphic rocks (e.g., Batt et al., 2001).

The composite samples of the Otago Schist (Fig. 1, 17 composites from Torlesse terrane and four composites from the Caples terrane) were collected using a traverse sampling technique in order to measure bulk compositions of whole outcrops as a function of metamorphism (Breeding and Ague, 2002). In this method, representative samples (~3–16 kg) were collected at regular intervals along a measuring tape laid out at a high angle to lithologic layering or foliation. The average traverse was ~50-meters long and comprised 26 samples. After pulverizing, two grams of each of the 26 samples were

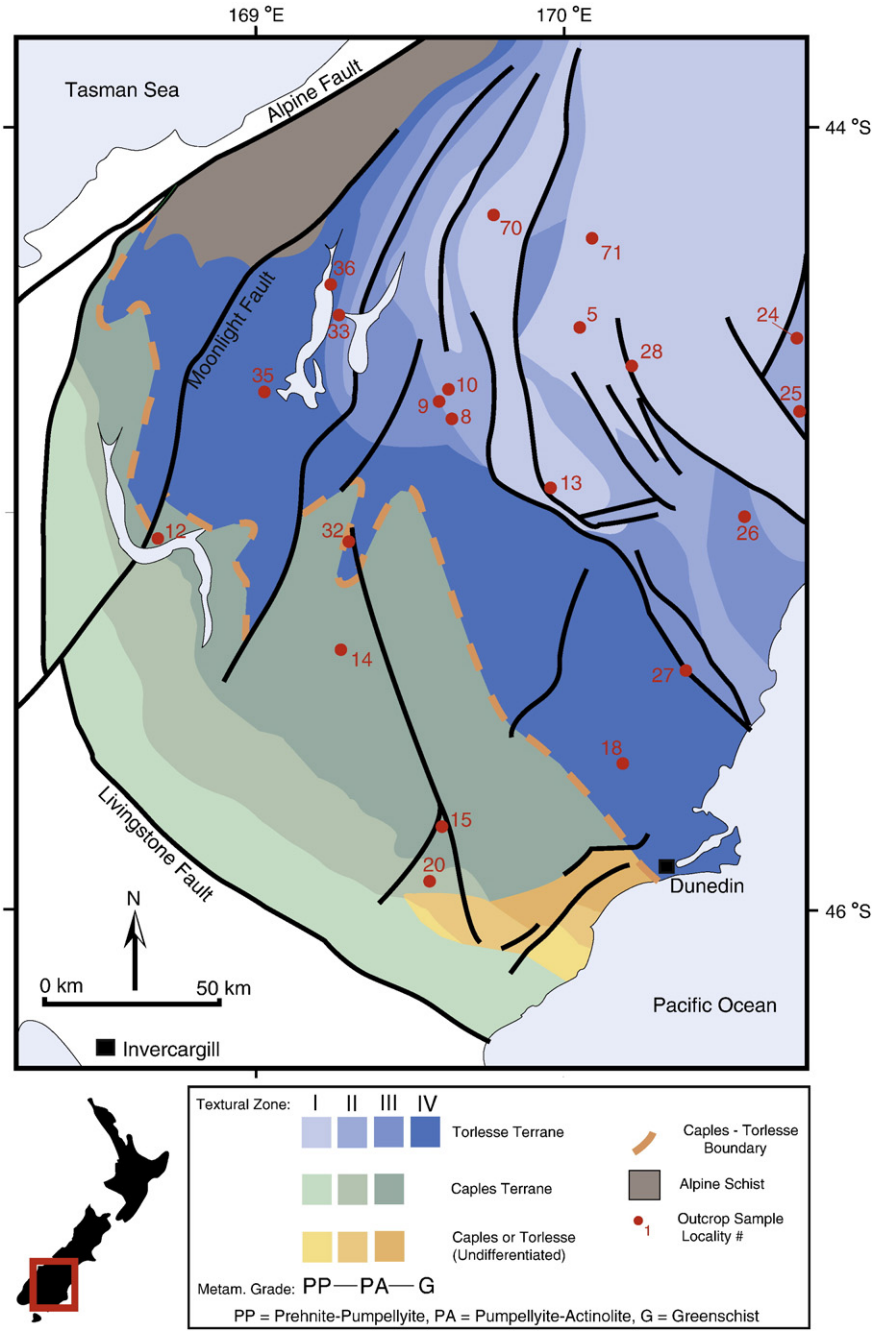

Fig. 1. Sketch map showing the sample location of Otago Schist, New Zealand (from Breeding, 2004). "Texture zones" indicate the degree of macroscopic deformation textures of the minerals, with zone I being least deformed and zone IV being most deformed (Breeding, 2004).

mixed to form the outcrop composite (Breeding and Ague, 2002). The sub-greenschist and greenschist facies samples are characterized by meta-graywacke and metapelitic assemblages, mainly composed of quartz, albite, chlorite and muscovite, with small amounts of calcite, epidote, and stilpnomelane; the sub-greenschist facies samples also contain ~15 vol.% of prehnite and pumpellyite. The disappearance of prehnite and pumpellyite and the appearance of clinozoisite marks the change from sub-greenschist to greenschist facies metamorphism (Bishop, 1972).

Relatively undeformed sub-greenschist facies samples are nearly vein-free and are traditionally considered as the precursor lithologies of the greenschist facies metamorphic rocks, which are highly deformed and contain significant amounts of veins (up to 30 vol.%) composed primarily of quartz, with lesser amounts of albite, calcite and clinozoisite. According to Breeding and Ague (2002), the greenschist facies outcrops can be divided into three groups. Seven of 10 sampled outcrops (referred to herein as Group A) have experienced mass addition of externally derived silica, interpreted to be deposited from slab-derived fluids originating from the deep prism; one outcrop, in the Macraes Flat area Au–W deposit (referred to herein as Group B), was probably flushed with retrograde metamorphic fluids from relatively shallow depths (De Ronde et al., 2000) or disturbed by later short-lived thermal events (Mortensen et al., 2010). The remaining two outcrops (referred to herein as Group C) contain veins of locally derived silica and may have experienced mass loss. While we present data for all groups, we primarily focus on Group A, as this group likely provides more detailed information about Li behavior during fluid fluxing. Several quartz veins in Group A outcrops, which are coarse enough to be separated completely, were manually cut from the wallrocks and analyzed in order to investigate the Li signature of the fluids (see Appendix A for photos of the veins and thin sections).

3. Methods

Lithium concentration and isotopic compositions of the composites and selected quartz veins were determined at the Geochemistry Laboratory of the University of Maryland, College Park. Sample dissolution procedures, column chemistry and instrumental analysis are reported in Qiu et al. (2009) and Teng et al. (2006). Briefly, samples were dissolved in a screw-top teflon beaker with a combination of HF–HNO_3–HCl. Lithium was purified on a cation exchange resin (Bio-Rad AG50w-X12, 200–400 mesh) first in an HCl medium, followed by an HCl-ethanol medium. Lithium concentrations and isotopic compositions were analyzed using the standard-sample-bracketing method on a Nu Plasma MC-ICPMS. One measurement of the rock reference material BCR-1 gives $\delta^7Li = 2.2$ and [Li] = 12.7 μg/g; as a benchmark, Magna et al. (2004), Rudnick et al. (2004) and Teng et al. (2006), reported the δ^7Li of BCR-1 to be 2.0 ± 0.7 (10 runs), $\delta^7Li = 2.7 \pm 1$ (3 runs) and $\delta^7Li = 2.4 \pm 0.5$ (4 runs), respectively, and GEOREM (Jochum and Nohl, 2008) preferred BCR-1 [Li] = 13 ± 1 μg/g. The long-term external precision of the Li isotopic composition and concentration analyses are ≤1.0‰ (2σ) and ±10% (2σ), respectively, based on repeat analyses of pure Li standards and standard reference materials, respectively, over the past nine years (Teng et al., 2006).

4. Results

Lithium concentrations and isotopic compositions are reported in Table 1, along with the major and trace elements of the composites from Breeding and Ague (2002). The [Li] in the sub-greenschist facies composites vary from 26 to 48 μg/g (Fig. 2), with an average of 41 ± 13 μg/g (2σ). The [Li] in the Group A greenschist facies composites show a lower and narrower range (25 to 40 μg/g), with an average of 34 ± 9 μg/g (2σ), which is statistically distinct from sub-greenschist facies composite at the 97.7% confidence level, as indicated by the univariant Student's t-test. Both data populations have a normal distribution, with negligible differences in their respective values of average, median and log-normal average. The Au–W deposit composite of Group B has the highest [Li] measured in any of the sub-greenschist and greenschist facies samples of 55 μg/g, whereas the two composites in Group C have a relatively large variation in [Li] of 26 and 48 μg/g. In contrast to the variable Li concentration observed between sub-greenschist and greenschist facies composites, the δ^7Li of both sample suites are statistically indistinguishable (Student's t-test); the average δ^7Li of the sub-greenschist and greenschist facies composites is 0.2 ± 1.7 (2σ) and -0.5 ± 1.6 (2σ), respectively (Fig. 2). The selected quartz veins from the Group A outcrops show [Li] and δ^7Li in the range of 0.4 to 2.3 (μg/g) and −2.8 to −1.4, respectively.

5. Discussion

5.1. Factors controlling [Li] in the greenschist facies composites

The Chemical Index of Alteration (CIA, see Table 1 for definition) is a useful way of quantifying the degree weathering in the source regions of sedimentary rocks (Nesbitt and Young, 1982) and generally shows a positive correlation with [Li] (Qiu et al., 2009). The [Li] in all groups of composites correlates with their CIA (values between 50 and 58, Fig. 3). The Otago Schists plot at the lower end of the trend defined by pelites from the British Caledonides (Qiu et al., 2009), consistent with their inferred graywacke protolith and indicating that the [Li] in the protolith has a great control on the [Li] of the Otago Schist. Other factors that may influence [Li] in these rocks, such as metamorphism and dilution due to quartz vein precipitation are considered next.

The fluids from which the quartz veins precipitated in the greenschist facies Group A composites are inferred to be Na-rich, K-poor and silica-saturated (Breeding and Ague, 2002); consequently, insoluble elements, like Zr, are diluted by the mass addition of quartz veins (Breeding and Ague, 2002). The dilution effect for any element can be investigated by correlations with an immobile reference element in a wedge diagram (Ague, 1994; Philpotts and Ague, 2009), a graphical way to assess the mass change (i.e., addition or dilution) in altered rocks relative to the precursor rocks. In these diagrams, a wedge-shaped region is defined between the origin and the precursor rock compositions (traditionally, the immobile reference element and studied element are plotted on the x- and y-axis, respectively). Altered rocks experienced dilution if they plot in the wedge-shaped region between the origin and the precursor rocks (Ague, 1994; Philpotts and Ague, 2009).

Figure 4 demonstrates that Group A composites (gray cloud) plot between the origin and sub-greenschist facies composites (blue cloud) for Al and Zr, two fluid-immobile elements. Further, using the two-dimensional Kolmogorov–Smirnov (2DKS) test (Press et al., 1992), the difference between these two groups is statistically significant at the 98.5% confidence level. Therefore, in Group A samples, Al, like Zr, has been diluted and can be used as a reference immobile element in a wedge diagram.

In order to constrain the dilution effect for Li, both Al and Zr are employed as immobile reference elements in two wedge diagrams. The plots of Li vs. Al (Fig. 4b) and Li vs. Zr (Fig. 4c) show that Group A composites plot between the origin and the sub-greenschist facies composites in the two wedges. Furthermore, the two groups in the two plots differ at the 99.8 and 97.1 confidence levels (2DKS test), respectively. These results indicate that, in the Group A composites, Li has also been diluted by mass addition of externally derived silica, consistent with the low [Li] of the quartz veins ([Li] ≤ 2.3 μg/g). By contrast, the Group B composite, which has the highest [Li] of any of the samples at 55 μg/g, plots above the wedge, indicating that it experienced enrichment in [Li]. Li may have been added from retrograde metamorphic fluids or hydrothermal fluids that contributed to the mineralization

Table 1
Lithium concentrations (μg/g), isotopic compositions, and major (wt.%) and trace elements (μg/g) data for Otago Schist composites.

		Sample	NZ grid reference	Li (mg/g)	δ^7Li	Mass A.	SiO_2	TiO_2	Al_2O_3	Fe_2O_3	MnO	MgO	CaO	Na_2O	K_2O	P_2O_5	LOI	LOI*	Total	CIA	Rb	Sr	Zr	Ba	W
Sub-greenschist facies		JANZ-5	H39 699340	47	0.1	/	63.3	0.73	16.2	5.71	0.09	2.16	2.78	3.25	2.05	0.17	3.40	3.40	99.8	57	88	240	164	442	0.58
		JANZ-8	G40 335023	41	0.0	/	66.0	0.62	15.3	4.20	0.06	1.60	2.42	3.39	2.70	0.16	2.15	2.15	98.6	55	109	308	222	585	/
		JANZ-9	G40 315068	48	0.4	/	67.0	0.57	15.4	4.12	0.07	1.44	2.30	3.78	2.87	0.13	2.10	2.10	99.8	54	105	317	212	667	/
		JANZ-10	G40 316067	43	−0.6	/	66.9	0.59	15.0	4.15	0.07	1.58	2.13	3.85	2.67	0.11	1.90	1.90	98.9	54	98	287	203	688	0.15
		JANZ-13	H41 653881	47	2.6	/	64.3	0.64	16.1	4.75	0.07	1.97	2.40	3.44	2.90	0.17	2.20	2.20	98.9	56	109	386	177	629	0.49
		JANZ-20	G44 373719	47	−0.3	/	66.3	0.63	15.8	4.07	0.06	1.42	1.62	3.52	3.39	0.15	2.20	2.20	99.2	57	126	191	205	608	0.28
		JANZ-24	I39 280295	34	0.4	/	65.3	0.64	15.7	4.62	0.08	1.89	2.75	3.44	2.55	0.17	2.70	2.70	99.8	55	103	238	188	594	0.43
		JANZ-25	J39 323104	26	−0.5	/	66.0	0.60	15.8	3.82	0.07	1.50	2.33	3.83	3.05	0.16	1.90	1.90	99.1	54	98	338	198	662	0.64
		JANZ-28	H39 867235	36	−0.5	/	62.4	0.76	16.6	6.11	0.08	1.93	2.41	2.97	2.72	0.16	3.00	3.00	99.1	58	99	285	155	476	0.64
		JANZ-70	H38 528595	42	0.0	/	65.6	0.60	15.8	4.38	0.07	1.74	2.50	3.32	2.86	0.17	2.65	2.65	99.7	55	108	496	185	708	0.59
		JANZ-71	H38 759517	41	0.0	/	64.4	0.71	15.5	5.09	0.07	2.22	2.99	3.16	2.40	0.19	2.35	2.35	99.1	54	92	365	178	523	0.47
greenschist facies	A	JANZ-12	E41 650637	40	−2.4	5%	63.8	0.66	15.1	5.53	0.09	2.07	3.93	3.57	1.78	0.17	2.35	1.98	99.1	52	63	344	145	477	0.16
		JANZ-15	G44 400820	25	−0.1	11%	70.5	0.48	13.4	3.15	0.06	1.11	2.13	4.31	2.21	0.09	1.65	1.65	99.1	50	84	130	197	470	0.37
		JANZ-18	H43 840096	35	−1.0	5%	68.1	0.51	14.4	3.68	0.06	1.31	1.96	3.77	2.23	0.12	2.25	2.25	98.4	55	91	261	201	502	0.10
		JANZ-26	I41 182821	37	−0.2	4%	65.0	0.63	15.6	4.87	0.07	1.99	2.45	3.29	2.47	0.15	2.90	2.90	99.4	56	101	232	166	539	0.19
		JANZ-32	G41 118657	32	0.4	6%	68.2	0.52	14.2	3.74	0.05	1.51	2.58	3.62	2.48	0.13	2.20	2.20	99.2	52	90	406	188	627	0.16
		JANZ-33	F39 073337	37	−0.6	8%	67.2	0.57	15.2	4.34	0.07	1.53	2.49	3.57	2.33	0.12	2.25	2.25	99.7	55	91	300	169	662	0.14
		JANZ-36	F39 063395	35	0.1	4%	65.2	0.69	14.7	5.59	0.10	2.33	3.58	3.88	1.76	0.17	1.70	1.70	99.7	50	58	352	164	484	0.14
	B	JANZ-27	I42 105336	55	−0.2	3%	64.1	0.75	15.3	5.81	0.08	2.30	1.97	3.28	2.32	0.18	3.20	3.20	99.3	58	81	200	160	558	0.43
	C	JANZ-14	G43 190301	26	−0.8	−2%	60.1	0.81	16.2	6.46	0.10	2.69	5.06	3.67	1.83	0.18	1.90	0.72	99.0	54	56	453	150	517	0.11
		JANZ-35	F40 913095	48	0.0	−2%	63.9	0.67	15.3	5.35	0.11	1.75	2.13	3.12	2.16	0.15	4.60	4.60	99.2	58	97	179	184	551	0.07
	Qtz veins	JANZ12Q	E41 650637	0.4	−2.8																				
		JANZ32Q	G41 118657	2.3	−1.7																				
		JANZ33Q	F39 073337	1.7	−1.4																				

A, B and C indicates different groups in greenschist facies composite.
Mass A.: Mass Addition.
Grid reference, mass addition value, major (%) and trace elements (ppm) data are from Breeding and Ague (2002).
$CIA = Al_2O_3/(Al_2O_3 + CaO^* + Na_2O + K_2O) \times 100$ (molar contents, with CaO^* being CaO content in silicate fraction of the sample).
At least two aliquots (~25 mg each) of each composite sample were digested and put through the column chemistry procedures.
One aliquot (~50 mg) of each quartz vein sample was digested and put through column chemistry.
The Li data reported in this study represent the averages of ≥3 measurements of each composite sample, and ≥2 measurements of each quartz vein sample.
The uncertainties for [Li] (mg/g) and d7Li are ±10 (2 s) and ±1 (2 s), respectively.

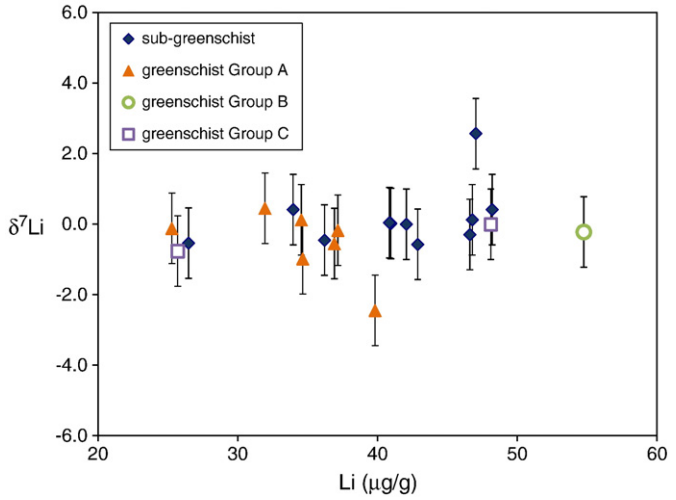

Fig. 2. Li isotopic composition (δ^7Li) versus Li concentration ([Li]) for the Otago Schist composites. Error bars represent 2σ uncertainty in the y-axis only. Uncertainties (2σ) in the x-axis are 10% of the concentration.

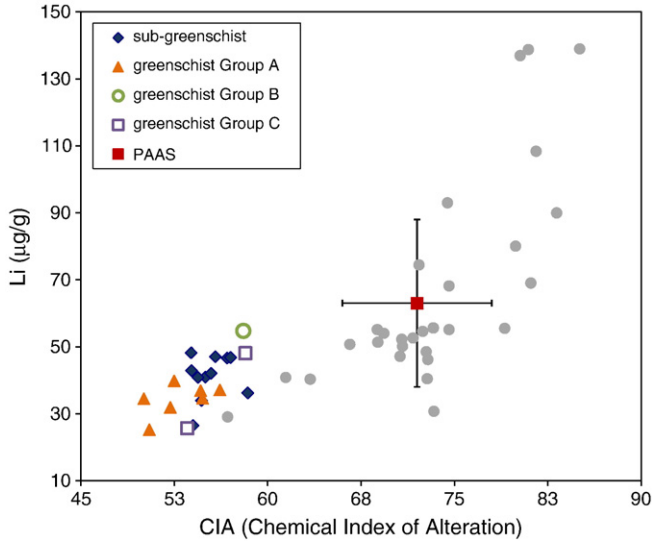

Fig. 3. Li concentration versus CIA (Chemical Index of Alteration) value for the Otago Schist composites. The gray dots are the British mudrocks from Qiu et al. (2009). PAAS: Post Archean Australian Shales. Average [Li] and CIA value of PAAS (with 1 σ uncertainty of the average) are according to Teng et al. (2004).

in this region. The two Group C composites show a large variation in [Li] and plot on the upper and lower bounds of the wedge within the field of sub-greenschist facies composites. There is no obvious change in [Li] associated with dilution within this group.

Whether or not dilution was the only process producing the lower [Li] in the greenschist facies composites can be evaluated from the linear correlation between the [Li] of Group A composites (34 ± 9 μg/g, 2σ) and the percentage of mass addition, previously calculated by Breeding and Ague (2002) based on a statistical (bootstrap) mass balance calculation (Fig. 5). This plot indicates that [Li] in the precursor rocks (prior to any mass addition) is on the order of 45 μg/g, similar to the average [Li] in the sub-greenschist facies composites (41 ± 13 μg/g, 2σ) and in the range typical of shales and

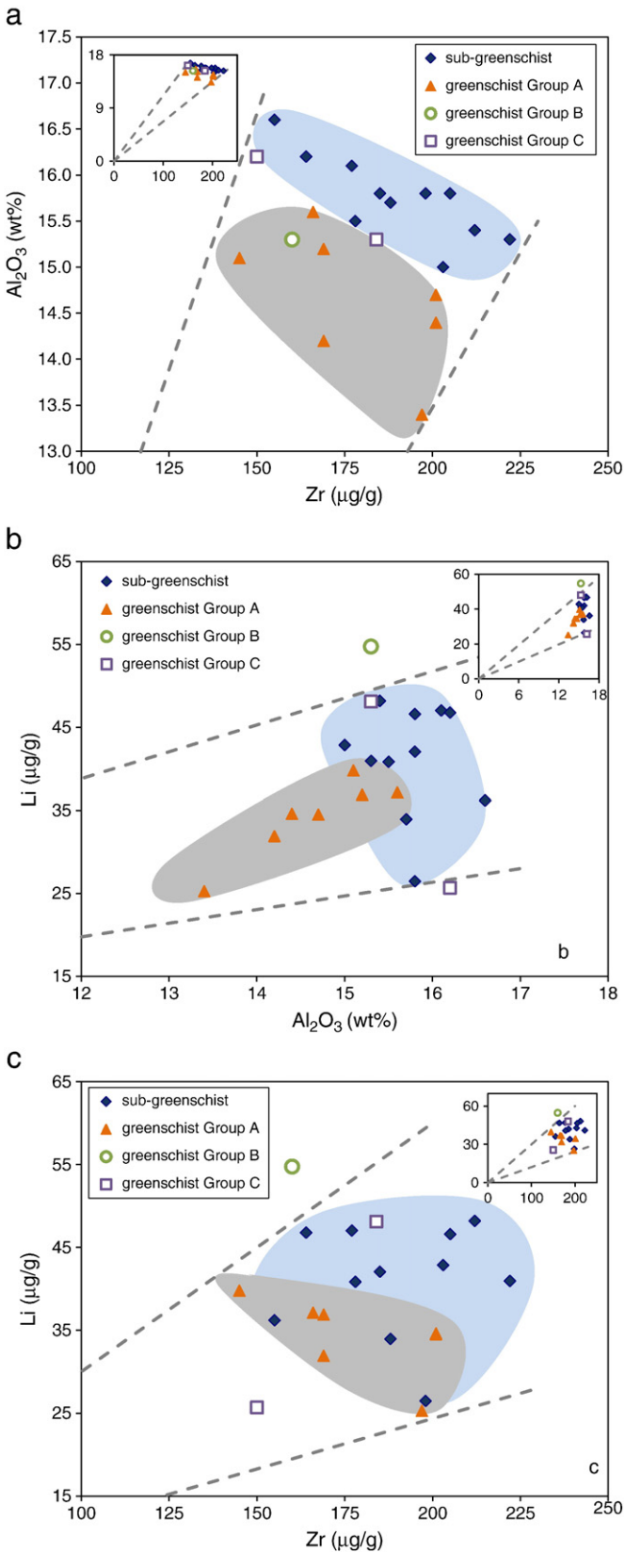

Fig. 4. Wedge diagrams of (a) Al_2O_3 versus Zr, (b) Li versus Al_2O_3 and (c) Li versus Zr for the Otago Schist composites. The wedge region (dashed lines) is projected from the origin, and elongated in order to include all the plots of precursor rocks (sub-greenschist facies composites in the blue cloud). The small plots in a, b and c are the full wedge diagrams showing axes extending to the origin. Note all altered rocks (greenschist facies Group A in the gray cloud) plot inside the wedge, and the trend from precursor rocks to altered rocks projects towards the origin, indicating a residual dilution effect (Ague, 1994; Philpotts and Ague, 2009). See text for details.

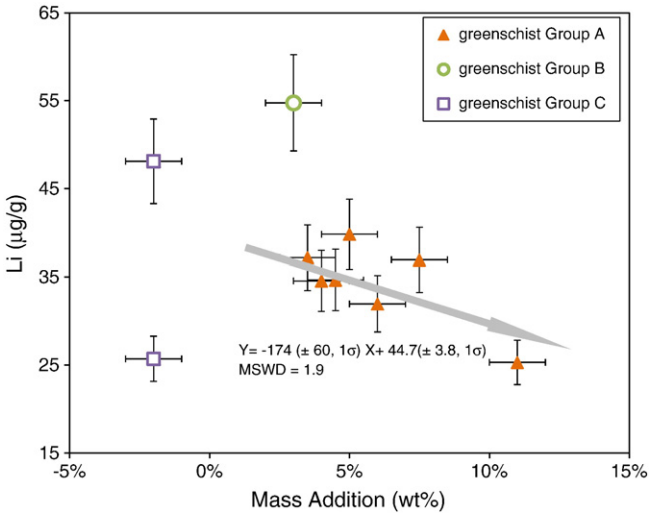

Fig. 5. Li concentration versus percent mass addition. The calculated mass addition and the horizontal error bars, which represent analytical variability in replicate composites, are from Figure 1B of Breeding and Ague (2002). The gray trend line and equation show the linear regression (calculated by Isoplot) between [Li] and mass addition.

graywackes (Qiu et al., 2009; Teng et al., 2004). Nevertheless, the mass addition of Li-depleted quartz veins cannot account for the total depletion of [Li] observed in the Group A composites, since the percentage of [Li] depletion does not match the percentage of calculated mass addition. For example, assuming ~45 μg/g Li in the Group A protolith, the abundance of Li in composite JANZ15 (25 μg/g) requires ~40 wt.% mass addition, whereas the calculated mass addition is only ~10 wt.%; therefore, another process must also have caused depletion of Li in the Group A samples.

Metamorphic dehydration has been implicated as a process that can cause Li depletion (e.g., Marschall et al., 2007; Teng et al., 2007; Zack et al., 2003). Although Qiu et al. (2009) established that [Li] in sub-greenschist facies mudrocks do not change systematically as a function of H_2O loss, sub-greenschist facies metamorphism may represent the lower boundary for Li depletion during metamorphism. Accordingly, higher grade metamorphism of metapelites may deplete Li during dehydration, as inferred from the results of Bea and Montero (1999) and Teng et al. (2007), which indicate that [Li] was depleted by ~50% during amphibolite facies metamorphism and 98% during granulite facies metamorphism, respectively. Therefore, dehydration accompanying greenschist facies metamorphism may also be capable of causing Li depletion. Consequently, greenschist facies metamorphism, together with mass addition, likely leads to the lower [Li] seen in Group A composites.

5.2. δ^7Li signatures

In contrast to [Li], the δ^7Li of sub-greenschist and greenschist facies composites are remarkably constant, averaging -0.1 ± 1.8 (2σ), which is indistinguishable from the value suggested for upper continental crust of 0.3 ± 2 (2σ; Teng et al., 2004) and overlapping with values observed in terrigenous turbidites and oceanic pelitic sedimentary rocks (δ^7Li = −1.6 to 5; Chan et al., 2006). Thus, there is no evidence for lithium isotopic fractionation during greenschist facies metamorphism, and the isotopic signatures of these metasediments likely reflect the δ^7Li of their protoliths.

The Li isotopic compositions of the quartz veins are surprisingly light (ranging from −2.8 to −1.4), given that quartz takes up ^{7}Li preferentially from fluids (Sartbaeva et al., 2004; Teng et al., 2006) and slab-derived fluids in the accretionary prism are suggested to have heavy δ^7Li signatures, up to ~ + 10 (Elliott et al., 2004; Tomascak, 2004 and references therein). If slab-derived fluids interacted with the wallrocks before the precipitation of the quartz veins, the fluids should be even heavier, because ^{7}Li preferentially partitions into fluids, similar to the effects of weathering (Chan and Edmond, 1988; Huh et al., 2004; Rudnick et al., 2004). Therefore, assuming that there are no other fluid sources contributing to quartz vein formation, the light δ^7Li of the quartz veins may record Li diffusion from Li-rich minerals in the wallrocks (e.g., chlorite, muscovite) into minerals in the veins. Such diffusion may occur in response to a chemical potential gradient between wall rock and vein, and may have been assisted by the presence of grain-boundary fluids, which have high partition coefficients for Li relative to rocks (e.g., Brenan et al., 1998). Since ^{6}Li diffuses faster than ^{7}Li (Dohmen et al., 2010; Richter et al., 2003; 2006), Li isotopes are fractionated during diffusion. Assuming that diffusion is arrested (i.e., the rocks do not fully equilibrate), this would produce quartz veins with low δ^7Li. Because the wall rocks have up to two orders of magnitude more [Li] than the quartz veins, small-scale diffusion may not influence the signature of Li in the wallrocks but may significantly change the δ^7Li of the quartz veins (Beinlich et al., 2010; Widmer and Thompson, 2001). As a result, the quartz veins likely do not reflect the isotopic signature of Li in the vein-forming fluids.

5.3. Isotopic equilibrium fluid flow model

The results above indicate that the slab-derived fluids have had no discernible effects on the δ^7Li of the schist composites. However, the dynamics of how the slab-derived fluid flux influences the δ^7Li of the overlying accretionary prism is still an open question. In order to investigate the extent to which slab-derived fluid flux might have affected the δ^7Li of the overlying greenschist-facies sediments, a one-dimensional local isotopic equilibrium model, following Dipple and Ferry (1992), has been applied. The MatLab code for the model is supplied in Appendix B and the equations used in the model are simply expressed as:

$$\delta^7 Li_{rock}(z,t) = \delta^7 Li_{fluid}\left(z - QN_f / V_r, 0\right) + \delta^7 Li_{rock}(z,0) - \delta^7 Li_{fluid}(z,0)$$

$$\delta^7 Li_{rock}(z,t) - \delta^7 Li_{fluid}(z,t) = \Delta_{rock-fluid}(T)$$

$$T = T_i + dT/dz * z$$

in which z is the distance along the flow path (cm), t is the time (s), Q is the time integrated flux (mol fluid/cm^2 rock), N_f (mol Li/mol fluid) and V_r (mol Li/ cm^3 rock) are the initial Li concentrations in the fluids and rocks, respectively, $\Delta_{rock\text{-}fluid}$ (T) is the temperature-dependent fractionation factor, T (K) is the temperature and T_i is the initial temperature at the crustal base, dT/dz (K/cm) is the temperature gradient along the flow path. The model also assumes that transport is by advection, and that diffusion and mechanical dispersion are negligible. Diffusion will operate locally (e.g., Penniston-Dorland et al., 2010), but mechanical dispersion can be important at regional length scales. If there was a significant component of mechanical dispersion, the geochemical fronts would be broader than shown, but the positions of the front mid-points would be unchanged.

The high grade Otago Schist records equilibration pressures equivalent to 25–30 km depth (Mortimer, 2003), which is relatively close to the higher end-member of the range of present day crustal thickness in this region (15–30 km, e.g., Davey et al., 2007; Stern et al., 2007); therefore, the crust could have been thicker at the time of fluid flow and we assume that the flow path region above the slab is 40 km thick. The results of our model indicate that the thickness of the crust does not significantly impact our model; for instance, by increasing the crustal thickness to 50 km, the maximum value of the [Li] in the fluids decreases slightly by ~2 μg/g, and decreasing the crustal thickness will not influence the [Li] of the fluids. The remaining variables include the

temperature at 40 km depth (the base of the crust), the initial δ^7Li and [Li] of the rocks and fluids, the temperature-dependent fractionation factor $\Delta_{solid\text{-}fluid}$, and the time-integrated fluid flux. Of these parameters, the temperature at the base of the crust and the temperature-dependent fractionation factor ($\Delta_{solid\text{-}fluid}$) have negligible influence on the δ^7Li of the sediments at 25—30 km depth (the derivation depth of the Otago Schist, Breeding and Ague, 2002). Changing temperature from 450 °C to 850 °C and adopting either the $\Delta_{solid\text{-}fluid}$-equation from Wunder et al. (2006, determined for low temperature basalt- seawater interactions), or the $\Delta_{solid\text{-}fluid}$-equation from Millot et al. (2010, determined for high temperature clinopyroxene-fluid interaction), results in <1‰ variation (i.e., within analytical uncertainties) in δ^7Li of the sediments. Therefore, we set the temperature at the base of the crust to 450 °C and use the isotopic fractionation equation ($\Delta_{solid\text{-}fluid}$) of Millot et al. (2010), since this equation is more suitable for our case, which is for whole rock–fluid systems.

The main contributors to the total Li flux in the model are the [Li] of the fluids and the time-integrated flux function. The time integrated flux is suggested to change over a narrow range (about one order of magnitude, from 27,000 to 144,000 m^3_{fluid}/m^2_{rocks}, as cited in Breeding and Ague, 2002), as compared to the range of the [Li] of the fluids from the prism (which may vary by two orders of magnitude, 0.1 – 10 μg/g, e.g., Chan and Kastner, 2000; Millot et al., 2010); thus, the variation of [Li] in the fluids has a greater impact on the model than does the time integrated fluid flux. We therefore set the integrated flux at 86,000 m^3_{fluid}/m^2_{rocks} (mean value of Breeding and Ague, 2002), in order to evaluate the impact of [Li] in the fluids. In contrast to the uncertainty of some of the input parameters above, the [Li] and δ^7Li of the sedimentary precursors are relatively well-established at 40 μg/g and 0, respectively, which is the Li signature of the sub-greenschist facies rocks of the Otago Schist, as well as typical graywackes (Teng et al., 2004). As a result, there are only two parameters that can be varied in the model to arrive at a range of acceptable solutions: the [Li] and the δ^7Li of the fluids.

The Li isotopic compositions observed in the greenschist facies Otago Schist ($\delta^7Li = -0.5 \pm 1.6$, 2σ) and the depth of the precursor sediments are shown as a field in Figure 6 (blue box). The curves in Figure 6a show the evolution of the δ^7Li of the rocks throughout the accretionary prism for four different model fluid compositions. The two green lines represent two isotopic equilibrium models with a Li-enriched fluid (13 μg/g Li), one having $\delta^7Li = 10$, and the other having $\delta^7Li = 1$. The two red lines represent the same models, but with a Li-depleted fluid (0.1 μg/g Li), one end-member with $\delta^7Li = 10$, and the other one with $\delta^7Li = 1$; the white arrow indicates the direction of the change of the curve in the box due to lowering [Li] of the fluids. When the fluid [Li]>13 μg/g, the model curve plots outside of the field defined by the greenschist facies Otago Schist, regardless of the δ^7Li of the model fluid. The more Li-depleted fluid models, however, intersect the Otago Schist field, even when the δ^7Li of the model fluid varies from 0 to > +30, suggesting that such fluids are potentially representative of the fluids that reacted with the Otago Schist protolith. The green lines in Figure 6a predict that shallower rocks should have noticeably lighter δ^7Li, which is not seen in the sub-greenschist facies Otago Schist. The constant δ^7Li of sub-greenschist to greenschist facies schist indicates the whole metamorphic sequence may not represent a connected flow system, or, the fluid flux becomes more channelized toward the surface and leaves the low-grade schist essentially unaltered. The discontinuities in both red and green lines in Figure 6a mark the position of the advective isotopic front; the sections above the discontinuity indicate that the sediments have not tapped the heavy isotopic front of the fluids, taking into account the temperature-dependent isotopic fractionation. Critically, however, there is no discontinuity in time-integrated fluid flux across the geochemical front. After reacting with the 40 km-thickness of sediments, the fluids ascending to the surface of the prism, regardless of their initial [Li] and δ^7Li, end up with heavy δ^7Li (>10, Fig. 6b) due to their interaction with the sediments. As

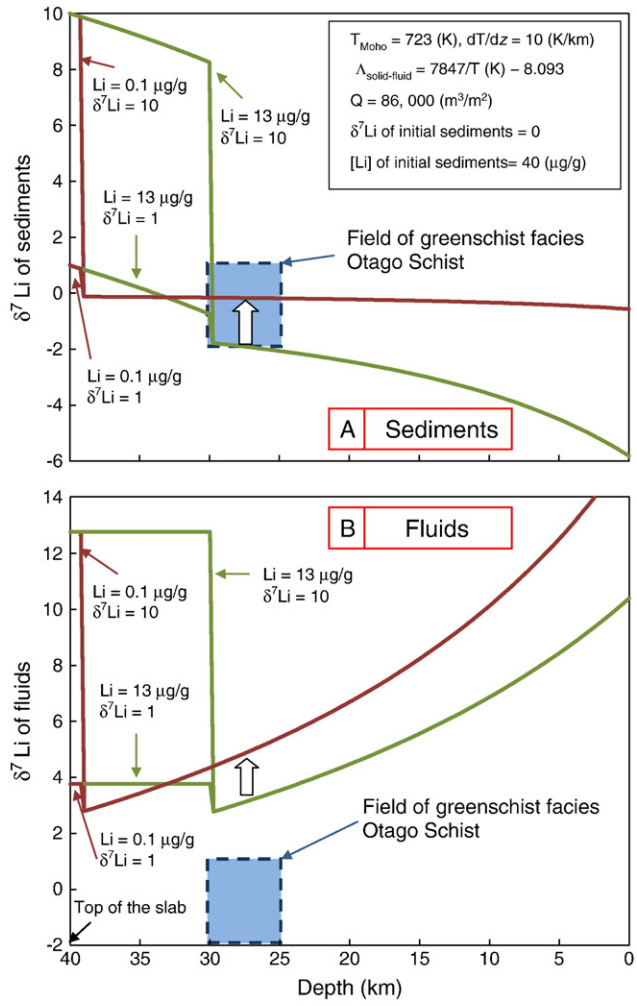

Fig. 6. Results of isotopic equilibrium fluid flow model (after Dipple and Ferry, 1992; calculated using a MatLab script, which is provided in Appendix B) showing (a) δ^7Li of the rocks and (b) fluids versus depth. Both red and green lines are calculated based on the assumptions that the temperature at the base of the crust is 450 °C, the fluid-rock isotopic fractionation is from Millot et al. (2010), the time integrated fluid flux is the mean of the values calculated by Breeding and Ague (2002) (86,000 m^3/m^2), and the initial [Li] and δ^7Li of the rocks are 40 μg/g and 0, respectively. The blue dashed box shows the field of the greenschist facies Otago Schist (25–30 km depth, $\delta^7Li = -0.5 \pm 1.6$, 2σ). The [Li] and δ^7Li of the model fluids are plotted next to the green and red lines, which indicate the results of modeling with high and low [Li] of the fluids, respectively. The white arrows indicate the direction that the curve moves as [Li] of the fluids decreases. Note that the isotope reaction front (i.e., the region at the base of the section where sediment compositions are overprinted with the isotopic composition of the fluids), generally propagates several kilometers upward from the slab into the overlying sediments. In this region the δ^7Li of the sediment closely follows the δ^7Li of the fluid, as indicated by the leftmost red and green curves on the upper panel. (See text for details).

expected, the Li-poor fluids (red lines) have heavier δ^7Li and less influence on the δ^7Li of the sediments than the Li-rich fluids.

The modeling results above were derived using a constant time integrated flux of 86,000 m^3_{fluid}/m^2_{rocks}; however, the time-integrated flux may vary between 27,000 to 144,000 m^3_{fluid}/m^2_{rocks} (Breeding and Ague, 2002). Using a time integrated flux lower than 86,000 m^3_{fluid}/m^2_{rocks}, allows the [Li] of the fluids to be higher than13 μg/g without changing the δ^7Li of the schists. For instance, if the time-integrated flux is set to the minimum value of 27,000 m^3_{fluid}/m^2_{rocks}, then the [Li] of the initial fluids will be $86{,}000(m^3_{fluid}/m^2_{rocks})/27{,}000(m^3_{fluid}/m^2_{rocks}) \times 13$ (μg/g) ≈ 41 (μg/g). This is the maximum value that can fit the δ^7Li of the Otago Schist data. The lower limit for [Li] in the fluids in our model is above ~0, i.e., the point where the δ^7Li of the sediments will be unchanged by fluids with low [Li]. The range of [Li] in the slab-derived

fluids from our model, $0<[Li]\leq 41$ (μg/g), is slightly lower than the modeling result of Marschall et al. (2007) for slab-derived fluid [Li] (~58 μg/g), which was calculated based on dehydration of average altered oceanic crust at 450 °C. Our range overlaps with the modeling results of Simons et al. (2010), $16<[Li]<43$ (μg/g), which were estimated based on the dehydration of 90% altered oceanic crust with 10% sediments at 450 °C.

In summary, although there are potentially a significant number of variables that can influence the equilibrium fractionation of Li between the fluid flux and the Otago Schist protolith, two variables, [Li] and δ^7Li of the fluids, are primarily responsible for the Li signatures observed in the Otago Schist, whose constant δ^7Li is best explained by interaction with a fluid depleted in Li (less than few μg/g), regardless of its isotopic composition. The total range of permissible [Li] in the fluids, $0<[Li]\leq 41$ (μg/g), overlaps with previous estimates of the composition of slab-derived fluids. Such fluids will have little influence on the δ^7Li of the sediments in the accretionary prism and will, in turn, be strongly influenced by their reaction with the sediments, such that their isotopic composition at the surface will be strongly altered from their original composition.

6. Conclusions

The [Li] and δ^7Li signatures of the Otago Schist indicate that, although prograde metamorphism from sub-greenschist facies to greenschist facies may have depleted the Li concentrations in these rocks, it had no discernible effect on the rocks' Li isotopic compositions. Further depletion of [Li] in greenschist facies composites is caused by mass addition of Li-poor quartz veins. The unusually low δ^7Li of the veins likely reflects preferential addition of ^{6}Li during Li diffusion into the veins from surrounding wall rocks. An isotopic equilibrium fluid flow model indicates that:

1) the δ^7Li of the precursor sediments of the greenschist-facies Otago Schist can be preserved after fluid fluxing if the [Li] in the fluid is relatively low;
2) the fluids have $\delta^7\text{Li} > +10$ when they approach the surface after reacting with the sediments;
3) the [Li] of the slab-derived fluids is in the range of $0<[Li]\leq 41$(μg/g); and
4) forearc fluids emerging at the surface may carry with them the compositional characteristics established during their interaction with prism sediments.

Supplementary materials related to this article can be found online at doi:10.1016/j.epsl.2010.11.001.

Acknowledgements

We thank M.T. Brandon, C.M. Breeding, N. Mortimer, J.M. Rahl, U. Ring, S. Penniston-Dorland and R. Arevalo for thoughtful discussions, D. MacPhee, P. Piccoli and R. Ash for their assistance in field and laboratory. The paper benefited from thoughtful review comments from Horst Marschall and Maureen Feineman and efficient editorial handling by Rick Carlson. This work was supported by NSF grants EAR 0609689 and 0948549 to Roberta L. Rudnick and William F. McDonough and 9814807 and 0105927 to Jay J. Ague.

References

Ague, J.J., 1994. Mass-transfer during barrovian metamorphism of pelites, South-Central Connecticut. 1: Evidence for changes in composition and volume. Am. J. Sci. 294, 989–1057.
Batt, G.E., Brandon, M.T., Farley, K.A., Roden-Tice, M., 2001. Tectonic synthesis of the Olympic Mountains segment of the Cascadia wedge, using two-dimensional thermal and kinematic modeling of thermochronological ages. J. Geophys. Res.-Sol. Ea 106, 26731–26746.
Bea, F., Montero, P., 1999. Behavior of accessory phases and redistribution of Zr, REE, Y, Th, and U during metamorphism and partial melting of metapelites in the lower crust: an example from the Kinzigite Formation of Ivrea–Verbano, NW Italy. Geochim. Cosmochim. Acta 63, 1133–1153.
Beinlich, A., Klemd, R., John, T., Gao, J., 2010. Trace-element mobilization during Ca-metasomatism along a major fluid conduit: eclogitization of blueschist as a consequence of fluid-rock interaction. Geochim. Cosmochim. Acta 74, 1892–1922.
Bishop, D.G., 1972. Progressive metamorphism from Prehnite–Pumpellyite to Greenschist Facies in Dansey Pass Area, Otago, New-Zealand. Geol. Soc. Am. Bull. 83, 3177–3198.
Breeding, C.M., Ague, J.J., 2002. Slab-derived fluids and quartz-vein formation in an accretionary prism, Otago Schist, New Zealand. Geology 30, 499–502.
Breeding, C.M., 2004. Fluid flow and mass transfer in subduction zones: A multi-scale view. Ph.D thesis. Yale University (AAT 3125163).
Brenan, J.M., Neroda, E., Lundstrom, C.C., Shaw, H.F., Ryerson, F.J., Phinney, D.L., 1998. Behaviour of boron, beryllium, and lithium during melting and crystallization: constraints from mineral-melt partitioning experiments. Geochim. Cosmochim. Acta 62, 2129–2141.
Chan, L.H., Edmond, J.M., 1988. Variation of lithium isotope composition in the marine-environment — a preliminary-report. Geochim. Cosmochim. Acta 52, 1711–1717.
Chan, L.H., Kastner, M., 2000. Lithium isotopic compositions of pore fluids and sediments in the Costa Rica subduction zone: implications for fluid processes and sediment contribution to the arc volcanoes. Earth Planet. Sci. Lett. 183, 275–290.
Chan, L.H., Leeman, W.P., Plank, T., 2006. Lithium isotopic composition of marine sediments *Geochem*. Geophys. Geosyst. 7. doi:10.1029/2005GC001202.
Davey, F.J., Eberhart-Phillips, D., Kohler, M.D., Bannister, S., Caldwell, G., Henrys, S., Scherwath, M., Stern, T., Avendonk, H.V., 2007. Geophysical structure of the Southern Alps Orogen, South Island, New Zealand. In: Okaya, D., Stern, T., Davey, F. (Eds.), A continental boundary: tectonics at South Island, New Zealand. : Geophysical Monograph Series, vol. 175. AGU, pp. 47–73.
De Ronde, C.E.J., Faure, K., Bray, C.J., Whitford, D.J., 2000. Round hill shear zone-hosted gold deposit, Macraes Flat, Otago, New Zealand: evidence of a magmatic ore fluid. Econ. Geol. 95, 1025–1048.
Dipple, G.M., Ferry, J.M., 1992. Fluid-flow and stable isotopic alteration in rocks at elevated-temperatures with applications to metamorphism. Geochim. Cosmochim. Acta 56, 3539–3550.
Dohmen, R., Kasemann, S.A., Coogan, L., Chakraborty, S., 2010. Diffusion of Li in olivine. Part I: Experimental observations and a multi species diffusion model. Geochim. Cosmochim. Acta 74, 274–292.
Elliott, T., Jeffcoate, A., Bouman, C., 2004. The terrestrial Li isotope cycle: light-weight constraints on mantle convection. Earth Planet. Sci. Lett. 220, 231–245.
Elliott, T., Thomas, A., Jeffcoate, A.B., Niu, Y., 2006. Lithium isotope evidence for subduction-enriched mantle in the source of mid-ocean-ridge basalts. Nature (London) 443, 565–568.
Huh, Y., Chan, L.H., Chadwick, O.A., 2004. Behavior of lithium and its isotopes during weathering of Hawaiian basalt. Geochem. Geophys. Geosyst. 5. doi:10.1029/2004GC000729.
Jochum, K.P., Nohl, U., 2008. Reference materials in geochemistry and environmental research and the GeoReM database. Chem. Geol. 253, 50–53.
Kerrich, R., 1999. Geochemistry — nature's gold factory. Science 284, 2101–2102.
Magna, T., Wiechert, U.H., Halliday, A.N., 2004. Low-blank isotope ratio measurement of small samples of lithium using multiple-collector ICPMS. Int. J. Mass Spectrom. 239, 67–76.
Marschall, H.R., Pogge von Strandmann, P.A.E., Seitz, H.M., Elliott, T., Niu, Y.L., 2007. The lithium isotopic composition of orogenic eclogites and deep subducted slabs. Earth Planet. Sci. Lett. 262, 563–580.
Millot, R., Scaillet, B., Sanjuan, B., 2010. Lithium isotopes in island arc geothermal systems: Guadeloupe, Martinique (French West Indies) and experimental approach. Geochim. Cosmochim. Acta 74, 1852–1871.
Mortensen, J.K., Craw, D., MacKenzie, D.J., Gabites, J.E., Ullrich, T., 2010. Age and origin of orogenic gold mineralization in the Otago Schist Belt, South Island, New Zealand: constraints from lead isotope and Ar-40/Ar-39 dating studies. Econ. Geol. 105, 777–793.
Mortimer, N., 1993. Jurassic tectonic history of the Otago Schist, New-Zealand. Tectonics 12, 237–244.
Mortimer, N., 2000. Metamorphic discontinuities in orogenic belts: example of the garnet-biotite-albite zone in the Otago Schist, New Zealand. Int. J. Earth Sci. 89, 295–306.
Mortimer, N., 2003. A provisional structural thickness map of the Otago Schist, New Zealand. Am. J. Sci. 303, 603–621.
Nesbitt, H.W., Young, G.M., 1982. Early Proterozoic climates and plate motions inferred from major element chemistry of Lutites. Nature 299, 715–717.
Penniston-Dorland, S.C., Sorensen, S.S., Ash, R.D., Khadke, S.V., 2010. Lithium isotopes as a tracer of fluids in a subduction zone mélange: Franciscan Complex CA. Earth Planet. Sci. Lett. 292, 181–190.
Philpotts, A.R., Ague, J.J., 2009. Principles of Igneous and Metamorphic Petrology, 2nd ed. Cambridge University Press, Cambridge, pp. 551–556.
Press, W.H., Teukolsky, S.A., Vetterling, W.T., Flannery, B.P., 1992. Numerical recipes in Fortran 77: The art of scientific computing, 2nd ed. Cambridge University Press, New York. 963 pp.
Qiu, L., Rudnick, R.L., McDonough, W.F., Merriman, R.J., 2009. Li and δ^7Li in mudrocks from the British Caledonides: metamorphism and source influences. Geochim. Cosmochim. Acta 73, 7325–7340.
Rahl, J.M., Brandon, M.T., Deckert, H., Ring, U., Mortimer, N., 2011. Tectonic significance of deformation in low-grade sandstones in the Mesozoic Otago subduction wedge. Am. J. Sci. 311. doi:10.2475/01.2011.01.

Richter, F.M., Davis, A.M., DePaolo, D.J., Watson, E.B., 2003. Isotope fractionation by chemical diffusion between molten basalt and rhyolite. Geochim. Cosmochim. Acta 67, 3905–3923.

Richter, F.M., Mendybaev, R.A., Christensen, J.N., Hutcheon, I.D., Williams, R.W., Sturchio, N.C., Beloso, A.D., 2006. Kinetic isotopic fractionation during diffusion of ionic species in water. Geochim. Cosmochim. Acta 70, 277–289.

Rudnick, R.L., Tomascak, P.B., Njo, H.B., Gardner, R.L., 2004. Extreme isotopic fractionation during continental weathering revealed in saprolites from South Carolina. Chem. Geol. 212, 45–57.

Sartbaeva, A., Wells, S.A., Redfern, S.A.T., 2004. Li^+ ion motion in quartz and beta-eucryptite studied by dielectric spectroscopy and atomistic simulations. J. Phys. Condens. Matter 16, 949–960.

Simons, K.K., Harlow, G.E., Brueckner, H.K., Goldstein, S.L., Sorensen, S.S., Hemming, N. G., Langmuir, C.H., 2010. Lithium isotopes in Guatemalan and Franciscan HP–LT rocks: Insights into the role of sediment-derived fluids during subduction. Geochim. Cosmochim. Acta 74, 3621–3641.

Smith, M.P., Yardley, B.W.D., 1999. Fluid evolution during metamorphism of the Otago Schist, New Zealand: (I) Evidence from fluid inclusions. J. Metamorph. Geol. 17, 173–186.

Stern, T., Okaya, D., Kleffmann, S., Scherwath, M., Henrys, S., Davey, F., 2007. Geophysical Exploration and Dynamics of the Alpine Fault Zone. In: Okaya, D., Stern, T., Davey, F. (Eds.), A Continental Boundary: Tectonics at South Island, New Zealand. : Geophysical Monograph Series, vol. 175. AGU, pp. 207–233.

Teng, F.Z., McDonough, W.F., Rudnick, R.L., Dalpe, C., Tomascak, P.B., Chappell, B.W., Gao, S., 2004. Lithium isotopic composition and concentration of the upper continental crust. Geochim. Cosmochim. Acta 68, 4167–4178.

Teng, F.Z., McDonough, W.F., Rudnick, R.L., Walker, R.J., Sirbescu, M.L.C., 2006. Lithium isotopic systematics of granites and pegmatites from the Black Hills, South Dakota. Am. Mineral. 91, 1488–1498.

Teng, F.Z., McDonough, W.F., Rudnick, R.L., Wing, B.A., 2007. Limited lithium isotopic fractionation during progressive metamorphic dehydration in metapelites: a case study from the Onawa contact aureole, Maine. Chem. Geol. 239, 1–12.

Tomascak, P.B., 2004. Developments in the understanding and application of lithium isotopes in the earth and planetary sciences. Geochem. NonTraditional Stable Isot. 55, 153–195.

Widmer, T., Thompson, A.B., 2001. Local origin of high pressure vein material in eclogite facies rocks of the Zermatt-Saas Zone, Switzerland. Am. J. Sci. 301, 627–656.

Wunder, B., Meixner, A., Romer, R.L., Heinrich, W., 2006. Temperature-dependent isotopic fractionation of lithium between clinopyroxene and high-pressure hydrous fluids. Contrib. Mineral. Petrol. 151, 112–120.

Zack, T., Tomascak, P.B., Rudnick, R.L., Dalpe, C., McDonough, W.F., 2003. Extremely light Li in orogenic eclogites: the role of isotope fractionation during dehydration in subducted oceanic crust. Earth Planet. Sci. Lett. 208, 279–290.